

Research of The New Soldering Alloys Based On Sn-Sr and Sn-Ag-Sr

Roman Kolenak¹, Alexej Pluhar², Igor Kostolny³, Jaromir Drapala⁴

^{1,2,3}Slovak University of Technology in Bratislava, Faculty of Materials Science and Technology in Trnava, Jana Bottu No. 2781/25, 917 24 Trnava, Slovak Republic

⁴FMMI – Faculty of Metallurgy and Material Engineering, 17. listopadu 15, Ostrava-Poruba, Czech Republic

²alexej.pluhar@stuba.sk

Abstract - The aim of the research was to characterize the soldering alloys type Sn1Sr and Sn3.5Ag1Sr. The DTA analysis of Sn1Sr solder has identified the eutectic reaction at the temperature of 232 °C. In the case of Sn3.5Ag1Sr solder, the eutectic reaction takes place at the temperature of 222 °C, which corresponds to the thermodynamic data for the given alloy type Sn-Ag-Sr. The microstructural SEM analysis has identified in soldering alloy type Sn1Sr the needles of primary precipitated intermetallic phase in the matrix formed of peritectic together with Sn, having majority proportion in the matrix. In the Sn1Sr solder, there was additionally observed the (Sn) + SrSn₄ eutectics with a high tin content. When analyzing the microstructure of Sn3.5Ag1Sr solder, the acicular constituents formed of ε-Ag₃Sn and Sr-Ag-Sn phases were observed. Also, the (Sn) + ε-Ag₃Sn eutectics was identified in solder volume. The solder matrix is formed of pure tin.

Keywords - active solder, microstructure, soldering, intermetallic phase, EDX analysis

I. INTRODUCTION

Due to the ban on the application of lead solders for joining the semiconductor parts in the electrotechnical industry, the research was oriented to the development of the new lead-free alloys [1-12]. The lead-free alloys exert a higher melting point and worse wettability when compared to the lead solders, which unfavorably affects the electric and mechanical properties. Due to that reason, the majority of lead-free alloys also contain a certain percentage of additional elements as Ag, Sb, Cu, etc. [13].

The most common lead-free solders comprise the Sn-based alloys with other additional elements. The Sn-Ag alloys may be considered for the widespread solders, which are broadly applied mainly for the soldering of semiconductor parts in electronics. Soldering with soldering alloys based on Sn-Ag with different alloying elements was also studied in works [14-19], where better results of adhesion and joint durability were attained in comparison with the lead solders and also good Ag properties regarding the joint strength. However, the melting point of Sn-Ag-based solders has exerted higher values when compared with the lead solders.

The Sn-Ag-based solders are also alloyed with a small amount of Ti as a special element since it is a highly chemically active element, which forms different intermetallic phases on the boundary with metallic substrates since it allows to join also the non-wettable materials as the ceramics of glass. It was found out that the addition of a small amount of Ti to Sn-Ag solder does not significantly affect the melting point, but it significantly improves the soldering properties [20,21]. The research is at present devoted also to strontium, which positive properties include the reduced shrinkage and porosity, but it also exerts some refining effect on several alloys [22]. Strontium is added to solders for improving the wettability of the ceramic but also metallic substrates.

The research work [23] deals with the development of new soldering alloys based on Al-Si-Zn-Sr destined for soldering the aluminum alloy type 6061. The effect of Sr on soldering alloy was studied. The results of the study have shown that Sr improved the wettability and strength of soldered joints. It similarly did not affect the melting point of the solder. The research has also shown that Sr addition resulted in a strong increase in overlapped joints by 14 % and by 11% in the case of butt joints.

Therefore, the aim of this work is to study the new soldering alloys based on Sn-Sr and Sn-Ag-Sr. The work is oriented to the structural study of solders. The characterization of solders was performed by the method of measuring the concentration of elements, as CP AES, DTA analysis of soldering alloys, and the microstructural SEM/EDX analysis.

II. EXPERIMENT

The weighing of individual components was done after determining the weight proportions of the prepared alloy as input components for solder manufacture were used materials with a high degree of purity (4N). Solder manufacture in as-cast condition was accomplished in a vacuum oven. The method was as follows: the charges of the alloy were inserted into a graphite boat. The boat contained with the charge was loaded into a tube made of siliceous glass, 59 mm in diameter. After that, the tube was placed into a horizontal vacuum resistance oven, which means it was



situated in the heating zone. If it is needed, the tube could be flushed with Ar through the flanges located on both ends. It is recommended to prepare this solder in Ar overpressure. After that, the entire charge was melted at the set temperature. Certain metals have good solubility in the base matrix. The dissolving and homogenization of solder components lasted around one hour while the solder was cooled down under free Ar protection. The formed alloy was melted again in a graphite crucible after removal from the oven and thoroughly stirred and cast into a graphite boat where it cooled very rapidly. Table 1 is given the composition of solders. ICP analysis, or Inductively Coupled Plasma is a powerful chemical analysis method that can be used to identify both trace amounts and major concentrations of nearly all elements within a sample. To determine the real elemental content of the solder was used, ICP AES analysis. The TG/DTA analysis of Sn1Sr and Sn3.5Ag1Sr solder was performed on the equipment type DTA SETARAM Setsys 18TM. The measuring system is provided with a cylindrical oven with a graphite heating element and appropriate control thermocouple, measuring rod, and the cooling medium. The crucibles made of Al_2O_3 inserted measured, and reference specimens were during experiment free laid on the measuring rod and were in contact with two thermocouples serving for the measurement of the difference in temperature between the measured and reference specimen. The heating rate of the specimen was $5\text{ }^\circ\text{C}/\text{min}$ from the room temperature up to the temperature of full melting of the specimen. This led to defining the temperatures of phase transformations in the liquidus-solidus range, phase transformation in solid-state, and the enthalpies of phase transformations were also determined. The solder specimen went through the standard metallographic procedure such as grinding, which was performed using SiC emery papers with the granularity of 240, 320, and 1200 grains/cm². Polishing was performed with diamond suspensions with $9\text{ }\mu\text{m}$, $6\text{ }\mu\text{m}$, and $3\text{ }\mu\text{m}$ grain sizes. Final polishing was accomplished using OP-S (Struers) polishing emulsion with $0.2\text{ }\mu\text{m}$ grain size. The solder microstructure was studied using scanning electron microscopy (SEM) on TESCAN VEGA 3 and JEOL 7600 F microscopes with a Microspec WDX-3PC X-ray micro-analyzer type to perform the qualitative and semi-quantitative chemical analysis.

III. RESULTS

A. The results of ICP AES analysis of soldering alloys

The results of measuring the specimens by the ICP AES method and the weighed amounts of solders are given in Table 1.

Table 1. The results of ICP AES analysis and the weighed amounts of solders

A weighed amount of solder			
Specimen No.	Sn [wt.%]	Ag [wt.%]	Sr [wt.%]
1. Sn1Sr	Base	-	1
2. Sn3.5Ag1Sr	Base	3,5	1
ICP AES analysis of solders			
Specimen No.	Sn [wt.%]	Ag [wt.%]	Sr [wt.%]
1. Sn1Sr	Base	-	0,97
2. Sn3.5Ag1Sr	Base	3,73	0,94

The average value of the element consisted of three measurements, whereas each element was identified individually. The results of analyses of alloying elements exert high reliability. The specimens were homogeneous, and the differences amongst the three measurements were minimum. The observations of ICP AES analyses have shown that the concentrations of Ag and Sr in alloys are in agreement with the weighed amounts of solders.

B. DTA analysis of soldering alloys

The results of the DTA analysis of soldering alloys are shown in Fig. 1. The specimens were during measuring process heated at the rate of $5\text{ }^\circ\text{C}/\text{min}$. Fig. 1 a) shows the result of measurement done by DTA analysis of Sn1Sr solder. The measurement has identified the only peak, which corresponds to eutectic reaction of Sn-Sr. The temperature of the eutectic reaction was identified at $232\text{ }^\circ\text{C}$. In accordance with the phase diagram of Sr-Sn, shown in Fig. 2, the equilibrium temperature of eutectic reaction is also $232\text{ }^\circ\text{C}$.

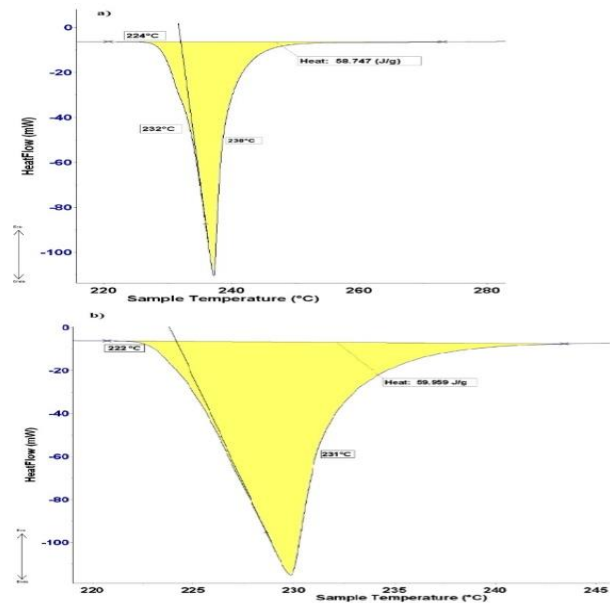


Fig. 1. a) DTA analysis of specimen No.1 - soldering alloy Sn1Sr; b) DTA analysis of specimen No.2 – soldering alloy Sn3.5Ag1Sr

Fig. 1 b) shows the result of measurement from DTA analysis of Sn3.5Ag1Sr solder. In accordance with the phase diagram of Ag-Sn (Fig. 3), the composition of Sn-Ag binary alloy at a concentration of 3.5 wt. % corresponds just to the eutectic point when the eutectic reaction takes place at 221 °C. The eutectic reaction for Ag-Sr system, at a concentration of 1 wt. % Sr takes place at the temperature of 231 °C. The temperature of the eutectic reaction detected at 222 °C by DTA analysis corresponds very well to the thermodynamic data for the given alloy type Sn-Ag-Sr. The eutectic reaction is connected with a significant thermal effect (60 J/g).

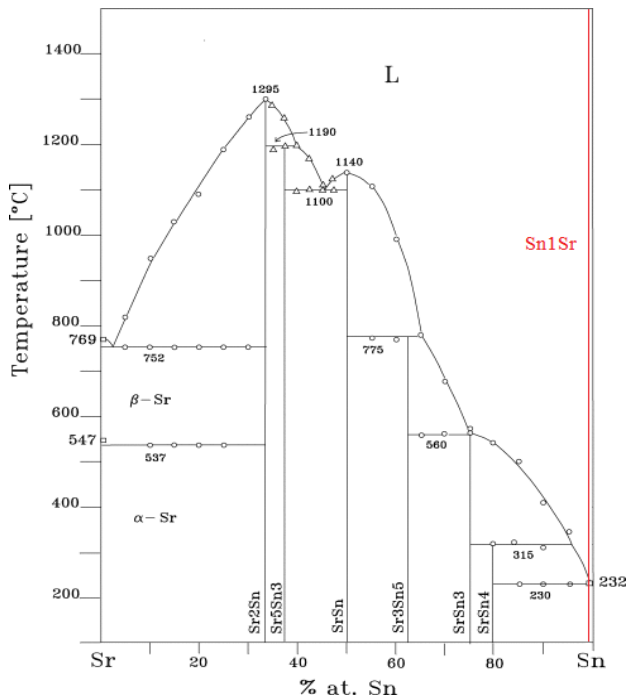


Fig. 2. Equilibrium binary diagram of Sr-Sn with a marked concentration of Sn1Sr solder [24]

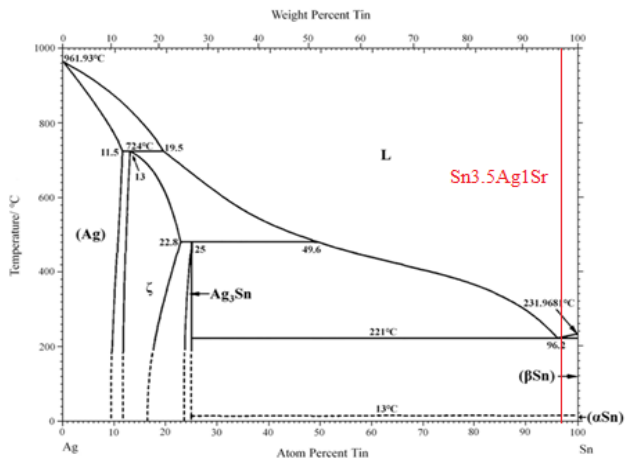


Fig.3 Equilibrium binary diagram of Ag-Sn with a marked concentration of Sn3.5Ag1Sr solder [25]

C. Microstructure of soldering alloys

The microstructure of Sn1Sr solder is shown in Fig. 4. The structure was observed by electron scanning microscopy (SEM) in BSE mode. The figure shows the needles of the primary segregated intermetallic phase in the matrix, formed of peritectic.

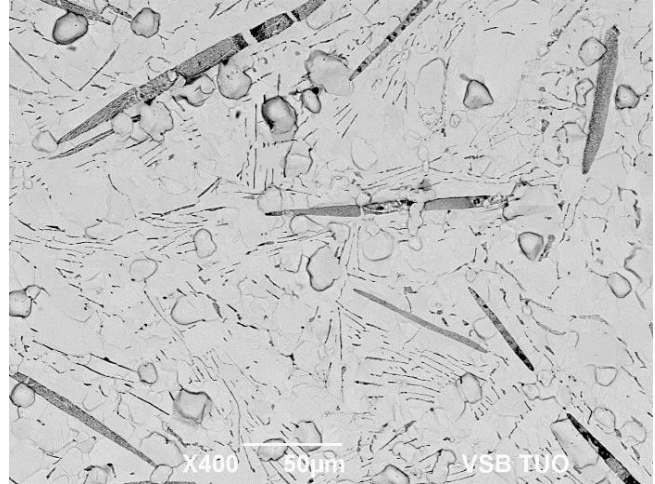


Fig. 4. Microstructural SEM analysis of Sn1Sr solder

The microstructure of Sn3.5Ag1Sr solder is shown in Fig. 5. The structure was observed by light microscopy. The structure shows the needles formed by Ag₃Sn and Sr-Ag-Sn phases.

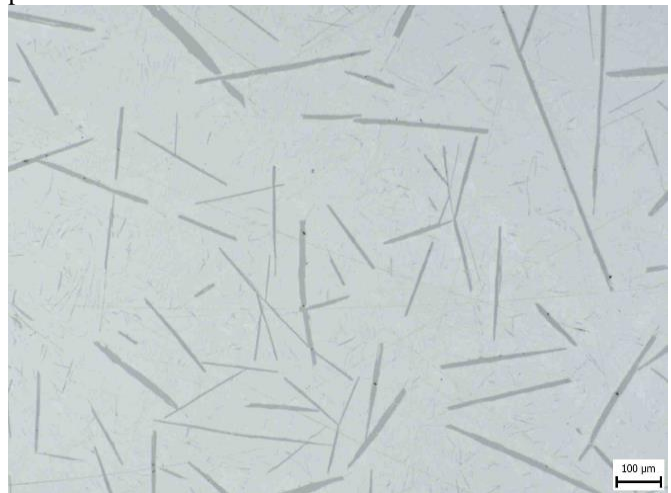


Fig. 5. Microstructural analysis of Sn3.5Ag1Sr solder performed by the light microscopy

D. EDX analysis of soldering alloys

Fig. 6 shows the map of elements where the components of Sn1Sr were identified. Strontium marked with violet color is contained in the acicular constituents together with Sn, marked by a yellow color, with majority proportion in them. The remaining part, besides the acicular constituents, is formed by tin. In order to prove these statements also point and planar analyses were performed in the given zone, as shown in Fig. 7. Their results are given in Table 2.

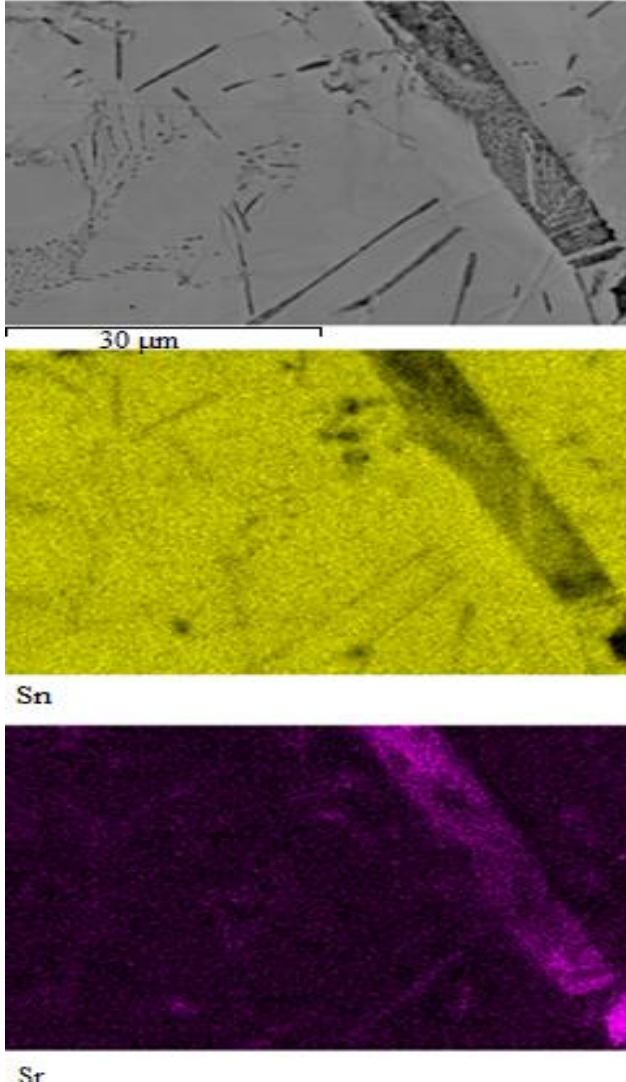


Fig. 6. Distribution of concentration of elements in Sn1Sr solder

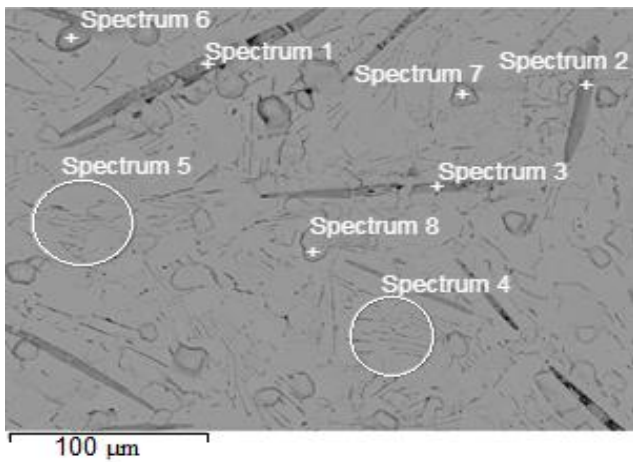


Fig. 7. EDX analysis of Sn1Sr solder

Table 2. The results of point and planar analyses of Sn1Sr solder

Spectrum	Sr [at.%]	Sn [at.%]	Solder component
Spectrum 1	5,3	94,7	phase SrSn ₄
Spectrum 2	5,7	94,3	phase SrSn ₄
Spectrum 3	6,5	93,5	phase SrSn ₄
Spectrum 4	0,1	99,9	eutectic (Sn) + SrSn ₄
Spectrum 5	0,3	99,7	eutectic (Sn) + SrSn ₄
Spectrum 6		100,0	pure Sn
Spectrum 7		100,0	pure Sn
Spectrum 8		100,0	pure Sn

In the shown spectra 1 to 3, the needles formed on an alloy composed of 94 at. % Sn and 6 at. % Sr may be observed. Those acicular constituents were formed at the primary crystallization. The marked zones of spectra 4 and 5 correspond to the matrix formed of pure tin, where fine needles of a phase enriched with Sr (planar analysis) occur – this concerns (Sn) + SrSn₄ eutectics with a high proportion of tin. In spectra 6 to 8, there are marked particles formed of pure tin. These observations are also proved by the work [24], supposing that at such a low Sr concentration, the SrSn₄ phase is present in the alloy.

The map of elements shown in Fig. 8. shows the identified components of Sn3.5Ag1Sr solder.

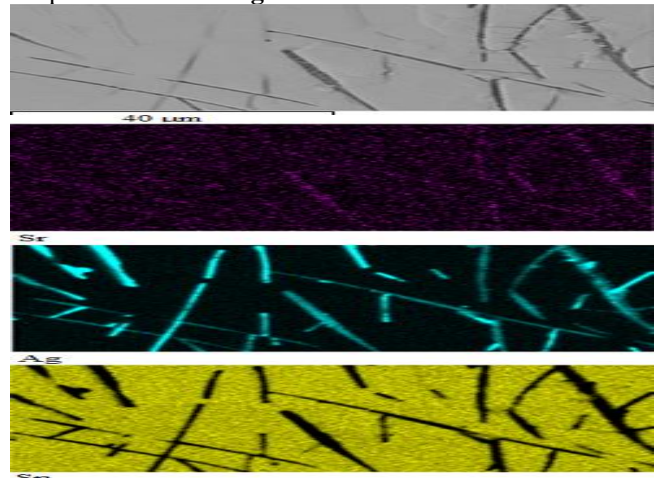


Fig.8. Distribution of concentration of elements in Sn3.5Ag1Sr

The blue color depicts the acicular constituents, which are in considerable measure formed of Ag; however, they also contain a certain percentage of Sr. The surroundings of those constituents are mostly formed of tin marked with yellow color. For a more precise specification of the given elements also the spot and planar analyses were performed, as shown in Fig. 9, and its results are given in Table 3.

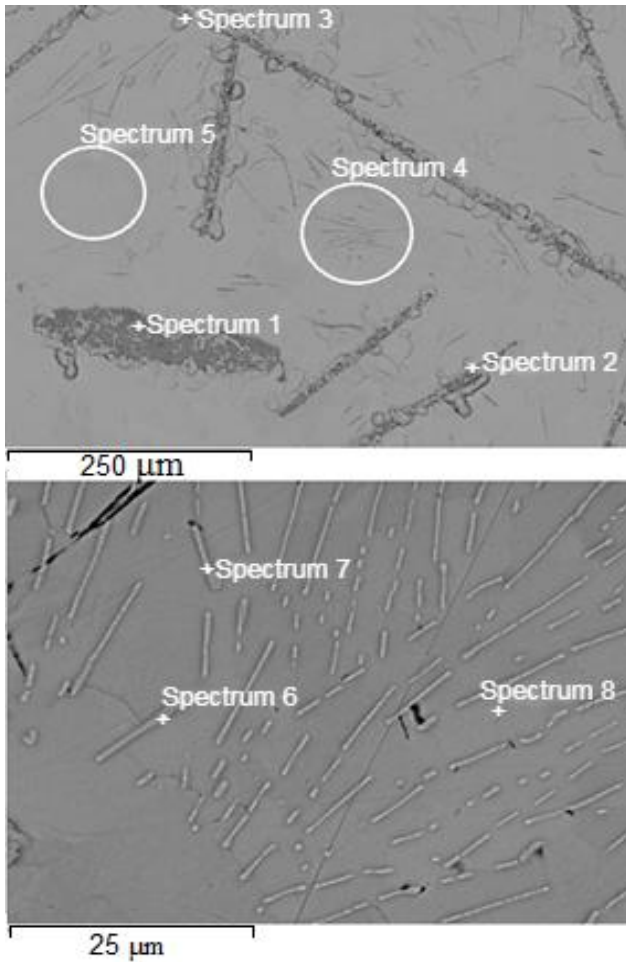


Fig.9. EDX analysis of Sn3.5Ag1Sr solder

Table 3. The results of point and planar analyses of Sn3.5Ag1Sr solder

Spectrum	Sr [at. %]	Ag [at. %]	Sn [at. %]	Solder component
Spectrum 1	20,4	47,1	32,5	phase Sr-Ag-Sn
Spectrum 2	20,4	34,6	44,9	phase Sr-Ag-Sn
Spectrum 3	17,6	39,4	43,1	phase Sr-Ag-Sn
Spectrum 4		2,9	97,1	eutectic (Sn) + ε-Ag ₃ Sn
Spectrum 5		1,8	98,2	eutectic (Sn) + ε-Ag ₃ Sn
Spectrum 6		69,0	31,0	phase ε-Ag ₃ Sn
Spectrum 7		68,2	31,8	phase ε-Ag ₃ Sn
Spectrum 8			100,0	pure Sn

The marked spectra 1 to 3 in Fig. 9 show the needles with different orientations formed of Sr-Ag-Sn phase with a high content of strontium and silver. The planar analysis of the zones in spectra 4 and 5 shows the areas with occurrence of (Sn) + ε-Ag₃Sn eutectics. The thin acicular constituents in spectra 6 and 7 in the Sn matrix correspond to ε-Ag₃Sn phase. The results of X-ray analysis are affected by the surrounding matrix, regarding the width of needles below 1 µm. The zone is marked. Spectrum 8 is formed of a matrix containing pure tin.

IV. CONCLUSION

The aim of the research was to characterize the new active soldering alloys type Sn1Sr and Sn3.5Ag1Sr. By experimental analyses, the following results were achieved:

- From the results of the ICP AES analysis, it follows that the concentrations of Ag and Sr in alloys are in agreement with the weighed amounts of solders.
- The DTA analysis of Sn1Sr solder has identified a reaction at the temperature of 232 °C. The results of measurement contain just one peak with identified eutectic reaction.
- The DTA analysis of Sn3.5Ag1Sr solder has shown that the eutectic reaction occurs at 222 °C, which corresponds to the thermodynamic data for the given alloy type Sn-Ag-Sr. Ag content in this alloy has reduced its melting point by 10 °C.
- Analyses of soldering alloy type Sn1Sr have revealed the needles of primary segregated intermetallic phase - (Sn) + SrSn₄. The solder matrix is formed of pure tin.

The needles of the Sr-Ag-Sn phase were identified in the structure of Sn3.5Ag1Sr solder, formed of a phase containing a high proportion of strontium and silver. The eutectic zones in solder are formed of (Sn) + ε-Ag₃Sn eutectics. The solder matrix is similarly formed of pure tin.

ACKNOWLEDGEMENT

This work was supported by the Slovak Research and Development Agency under contract no. APVV-17-0025. The paper was also prepared with the support of the VEGA 1/0303/20 project: Research of joining the metallic and ceramic materials in the production of power semiconductors.

REFERENCES

- [1] Sonawane P, Raja V.K, Palanikumar K, et al. Effects of gallium, phosphorus and nickel addition in lead-free solders: A review, Materialstoday: Proceedings, In press, Corrected proof.(2021).
- [2] Li Ch, Yan Y, Gao T, Xu G, The influence of Ag on the microstructure, thermal properties and mechanical behavior of Sn-25Sb-xAg high temperature lead-free solder, In Vacuum, 185 (2021).
- [3] Vafaenezhad H., Seyedein S.H., Aboutalebi M.R., et al. Creep life prediction for Sn-5Sb lead-free solder alloy: Model and experiment, In Microelectronic Engineering, 207 (2019) 55-65.
- [4] Chang S., Lin S., Hsieh K., Phase reaction in Sn-9Zn solder with Ni/Au surface finish bond-pad at 175 °C ageing, In Journal of Alloys and Compounds, 428 (2007) 179-184.

- [5] Kim D., Jung S., Interfacial reactions and growth kinetics for intermetallic compound layer between In-48Sn solder and bare Cu substrate, In *Journal of Alloys and Compounds*, 386 (2005) 151-156.
- [6] Jayesh S., Elias J., Investigations on the properties of new lead free alloy composition –Sn-0.5Cu-3.5Bi, In *materialstoday: Proceedings*, 21 (2020) 329-331.
- [7] Yang, L., Ma, S., Mu, G., Improvements of microstructure and hardness of lead-free solders doped with Mo nanoparticles, In *Materials Letters*, 304 (2021).
- [8] Shen, Y., Chen, S., Chen, H. et. al. Extremely thin interlayer of multi-element intermetallic compound between Sn-based solders and FeCoNiMn high-entropy alloy, In *Applied Surface Science*, 558 (2021).
- [9] Kanlayasiri, K., Ariga, T., Physical properties of Sn58Bi-xNi lead-free solder and its interfacial reaction with copper substrate, In *Materials & Design*, 86 (2015) 371-378 (2015).
- [10] Khodabakhshi, F., Zareghomsheh, M., Khatibi, G., Nanoidentation creep properties of lead-free nanocomposite solders reinforced by modified carbon nanotubes, In *Materials Science and Engineering:A*, 797 (2020).
- [11] Jung, D., Sharma, A., Jung, J., Influence of dual ceramic nanomaterials on the solderability and interfacial reactions between lead-free Sn-Ag-Cu and a Cu conductor, In *Journal of Alloys and Compounds*, 743 (2018) 300-313 (2018).
- [12] Zhang, L., Tu, K., Structure and properties of lead-free solders bearing micro and nano particles, In *Materials Science and Engineering: R: Reports*, 82 (2014) 1-32, (2014).
- [13] Pal M, Gergely G, Koncz-Horváth D, Gácsi Z, Investigation of microstructure and wetting behavior of Sn-3.0Ag-0.5Cu (SAC305) lead-free solder with additions of 1.0 wt% SiC on copper substrate, In *Intermetallics*, 128 (2021).
- [14] Šebo P, Švec P, Janičkovič D, Štefáňik P, Influence of thermal cycling on shear strength of Cu-Sn3.5AgIn-Cu joints with various content of indium, In *Journal of Alloys and Compounds*, 463(2008) 168-172.
- [15] Geranmayeh A.R., Nayyeri G., Mahumdi R., Microstructure and impression creep behavior of lead-free Sn-5Sb solder alloy containing Bi and Ag, In *Materials Science and Engineering:A*, 547(2012) 110-119.
- [16] Wiese S, Wolter K, Microstructure and creep behavior of eutectic SnAg and SnAgCu solders, In *Microelectronics Reliability*, 44 (2004) 1923-1931.
- [17] Schmitt P, Kaiser P, Savio C, et al. Intermetallic Phase Growth and Reliability of Sn-Ag Soldered Solar Cell Joints, In *Energy Procedia*, 27 (2012) 664-669.
- [18] Yao Y, Zhou J, Xue F, Chen X, Interfacial structure and growth kinetics of intermetallic compounds between Sn-3.5Ag solder and Al substrate during solder process, In *Journal of Alloys and Compounds*, 682 (2016) 627-633.
- [19] Keller J., Baither D., et al. Mechanical properties of Pb-free SnAg solder joints, In *ActaMaterialia*, 59(2011) 2731-2741.
- [20] Qu W., Zhou S., et al. Effect of Ti content and Y additions on oxidation behavior of SnAgTi solder and its application on dissimilar metals soldering, In *Materials & Design*, 88(2015) 737-742.
- [21] Tang Y., Li G., Thermodynamic Study of Sn-Ag-Ti Active Filler Metals, In *Physics Procedia*, 25(2012) 30-35.
- [22] Zhou B, Shang S, Liu Z, First-principles calculations and thermodynamic modeling of the Sn-Sr and Mg-Sn-Sr systems, In *Calphad*, 46(2014).
- [23] Dai W, Xue S, Lou J, Wang S, Development of Al-Si-Zn-Sr filler metals for brazing 6061 aluminium alloy, In *Materials & Design*, 42(2012) 395-402.
- [24] Palenzona A, Pani M, The phase diagram of the Sr-Sn system, In *Journal of Alloys and Compounds*, 384(2004) 227-230.
- [25] Hang, C., He, J., Zhang, Z. *et al.* Low Temperature Bonding by Infiltrating Sn3.5Ag Solder into Porous Ag Sheet for High Temperature Die Attachment in Power Device Packaging. *Sci Rep*8, 17422. <https://doi.org/10.1038/s41598-018-35708-6>, (2018).